PAPER

Investigating the role of low level reinforcement reflex loops in insect locomotion

To cite this article: C A Goldsmith *et al* 2021 *Bioinspir. Biomim.* **16** 065008

Bioinspiration & Biomimetics

PAPER

Investigating the role of low level reinforcement reflex loops in insect locomotion

RECEIVED
21 April 2021

REVISED
19 July 2021

ACCEPTED FOR PUBLICATION
21 September 2021

PUBLISHED
21 October 2021

C A Goldsmith[1,*], R D Quinn[2] and N S Szczecinski[1]

[1] West Virginia University, One Waterfront Place, Morgantown, WV 26506, United States of America
[2] Case Western Reserve University, 10900 Euclid Ave, Cleveland, OH 44106, United States of America
[*] Author to whom any correspondence should be addressed.

E-mail: cg00022@mix.wvu.edu

Keywords: synthetic nervous system, neuromechanical model, reflex reversal, desDUM neurons, non-spiking interneurons, femoral chordotonal organ

Supplementary material for this article is available online

Abstract

Insects are highly capable walkers, but many questions remain regarding how the insect nervous system controls locomotion. One particular question is how information is communicated between the 'lower level' ventral nerve cord (VNC) and the 'higher level' head ganglia to facilitate control. In this work, we seek to explore this question by investigating how systems traditionally described as 'positive feedback' may initiate and maintain stepping in the VNC with limited information exchanged between lower and higher level centers. We focus on the 'reflex reversal' of the stick insect femur-tibia joint between a resistance reflex (RR) and an active reaction in response to joint flexion, as well as the activation of populations of descending dorsal median unpaired (desDUM) neurons from limb strain as our primary reflex loops. We present the development of a neuromechanical model of the stick insect (*Carausius morosus*) femur-tibia (FTi) and coxa-trochanter joint control networks 'in-the-loop' with a physical robotic limb. The control network generates motor commands for the robotic limb, whose motion and forces generate sensory feedback for the network. We based our network architecture on the anatomy of the non-spiking interneuron joint control network that controls the FTi joint, extrapolated network connectivity based on known muscle responses, and previously developed mechanisms to produce 'sideways stepping'. Previous studies hypothesized that RR is enacted by selective inhibition of sensory afferents from the femoral chordotonal organ, but no study has tested this hypothesis with a model of an intact limb. We found that inhibiting the network's flexion position and velocity afferents generated a reflex reversal in the robot limb's FTi joint. We also explored the intact network's ability to sustain steady locomotion on our test limb. Our results suggested that the reflex reversal and limb strain reinforcement mechanisms are both necessary but individually insufficient to produce and maintain rhythmic stepping in the limb, which can be initiated or halted by brief, transient descending signals. Removing portions of this feedback loop or creating a large enough disruption can halt stepping independent of the higher-level centers. We conclude by discussing why the nervous system might control motor output in this manner, as well as how to apply these findings to generalized nervous system understanding and improved robotic control.

1. Introduction

Insects are excellent models in the study of locomotion. They are highly robust walkers, successfully navigating dynamic, uncertain terrains throughout their lives. Furthermore, their nervous systems are relatively small compared to larger vertebrates, allowing for more straightforward exploration of their various functions. These findings may then be extrapolated and scaled to larger organisms to establish commonalities in locomotion control.

Several aspects of the insect nervous system's control of locomotion have not yet been fully defined. In particular, precisely how the 'lower level' systems in the ventral nerve cord (VNC) communicate with 'higher level' systems in the head ganglia is

presently unknown [12, 33, 79]. Traditional experimental methods lack enough precision to definitively answer these questions; however, neuromechanical modeling can aid in bridging the gap. Presently difficult or impossible experiments can be run on morphologically accurate models to observe hypothetical outputs, and these models can be expanded based on functional behavior data to hypothesize certain network structures [26, 28, 53, 72, 77, 83]. These neuromechanical models can even be integrated into robotic test platforms with a high degree of biological fidelity to explore the role of mechanics and dynamics in nervous system behaviors [29, 37, 59]. Such models can then possibly serve as approachable guides for developing robots with similar motions by mimicking their neural processes, mechanics, and end behaviors, improving robotic capability in conjunction with neurobiological understanding [24, 42]. The main contribution of this work is to use a neuromechanical simulation 'in-the-loop' with a physical robotic test platform to explore how systems historically described as 'positive feedback' may control locomotion at the 'lower level' by reinforcing ongoing behaviors, with only sparse communication from the 'higher level'.

One feature of the nervous system that has been hypothesized as important to posture and locomotion control is the apparent 'reflex reversal' of insect joint control reflexes [16]. Briefly summarizing this behavior: stretching the femoral chordotonal organ (fCO) (signifying joint flexion) in an inactive, resting insect's femur-tibia (FTi) joint will result in a resistance reflex (RR) that attempts to halt the joint motion. However, in an active insect the same stimulus will cause an active reaction (AR), wherein the muscles allow the flexion to proceed [5, 38]. These two context-dependent responses to the same sensory stimulus highlight the flexibility of the nervous system.

The exact mechanisms in the nervous system that cause reflex reversal are as yet unidentified; however, several studies hypothesize the importance of groups of non-spiking interneurons (NSI) between the sensory neurons receiving stimuli from the fCO and the slow extensor tibiae motorneuron (SETi) [56, 57]. In particular, Sauer *et al* (in reference [55]) found that blocking Chlorine ion channels (which causes inhibition) in the VNC changes NSI responses and eventually the motor neuron (MN) responses to fCO stretching. Based on these results, the authors suggest that the nervous system may create reflex reversal by selectively inhibiting or disinhibiting fCO afferents present in the VNC. Driesang *et al* similarly found in reference [27] that NSI properties appear unchanged between the RR and the AR while NSI activity changes, implying it is their inputs (i.e. sensory afferent activity) that are changing.

If the sensory afferents are in fact being impinged upon to bring about reflex reversal, a new question arises: what mechanisms in the nervous system could reasonably cause this modulation? Several studies seem to indicate the importance of populations of descending dorsal unpaired median (desDUM) neurons, which are located in the posterior gnathal ganglion and send bilateral axons down into the thoracic ganglia [14, 19, 63, 64, 67]. These desDUM neurons are a major cellular source of the biogenic amine octopamine in the gnathal ganglion, a neuromodulator that acts as a homolog to noradrenaline in the invertebrate nervous system [32, 52]. Octopamine has previously been found to alter the activity of sensory organs such as the fCO in a variety of insects [15, 46, 49]. In particular, Büschges *et al* showed in reference [22] that bathing the animal's VNC in octopamine suppressed the RR and allowed the AR to occur. Stolz *et al* similarly found that activation of the desDUM neurons specifically increase the likelihood of reflex reversal (figure 9 in [68]). Considering these findings, it seems reasonable to assume that octopamine from the desDUM neurons contributes, in part, to reflex reversal in the FTi joint (but may not be the only mechanism).

As the AR occurs in 'active' insects, octopamine has also been observed to play a part in stimulating locomotion. Previous studies have shown that activity in the gnathal ganglion mediates locomotion (review in reference [31]). In neck-lesioned insects, the application of octopamine to the thoracic ganglia has been found to increase the likelihood and duration of walking bouts [50, 84]. Within the framework that rhythmic joint motion is driven by individual central pattern generators (CPGs) whose relative phasing is controlled by sensory feedback from the leg [6, 9, 11, 23, 45, 54], it seems reasonable to assume that octopamine or some other excitatory neuromodulator provides targeted, calibrated excitatory drive to sustain CPG oscillation [45, 48]. If octopamine increases walking activity in the thoracic ganglion, then the desDUM neurons potentially also activate the CPGs, and perhaps the MNs directly as well.

While the desDUM neurons have been continuously researched, their exact inputs are still unknown. Mentel *et al* found in reference [47] that desDUM populations would receive depolarizing synaptic input when the abdomen or antennae were mechanically stimulated, which implies inputs from elsewhere in the gnathal ganglia or higher up in the nervous system. The desDUM neurons would also receive this excitation when parts of the leg were mechanically stimulated [47]. Further, Stolz *et al* found that the desDUM neurons would be activated in stance phase during treadmill walking, and that the level of excitation would increase with the velocity of the treadmill (figure 3 in reference [68]). Combined with the Mentel *et al* results, this

behavior points toward the desDUM neurons receiving inputs corresponding to the strain of the leg, likely from campaniform sensilla (CS) load sensors [3, 21, 85, 86, 88].

Several nervous system models have investigated how these specific lower level systems give rise to walking. Bässler *et al* have previously attempted to functionally model reflex reversal in reference [7] and used the model for simulated joint control. However, because NSI sub-network morphology had not been characterized prior to the model's development, the system lacks these details. Sauer *et al* later traced the connectivity of the NSIs in reference [57] and developed a data-driven model of the sub-system, but neither used the model to control a limb or modified it to observe the response. Nearly a decade later, Stein *et al* replicated and expanded the Sauer network in reference [66] in order to explore modifications that would bring about reflex reversal in the network. However, they focused on modifying the strengths of the interneuronal pathways between the NSIs and the MNs over modulating the sensory afferents to achieve the desired effect, which is not supported by Sauer *et al* and Dreisang *et al* [27, 55]. They also did not include limb mechanics into their simulation. Some simulations have included mechanics [62], but the mechanisms they used to create reflex reversal were functional, not morphological. To our knowledge, no dynamic neuromechanical models of this particular sub-network currently exist from which to observe the closed loop joint behavior.

Furthermore, to our knowledge, no neuromechanical models of insect locomotion have considered how feedback from leg-local sensors might contribute to motor system 'drive' and the behavioral state of the animal. Many models investigate the bifurcation of networks from a quiescent to active (i.e. stepping or walking) state [4, 77]. In particular, we have previously developed a model to explore such questions [37]. However, in these models, descending drive is typically modeled as an applied synaptic current that does not depend on local network activity or sensory feedback. While other neuromechanical models have considered how an animal might autonomously transition between behavioral states, e.g. between static standing and active walking, such transitions have been driven by internal models and central mechanisms rather than by leg-local sensory feedback [60]. Furthermore, while such models can produce impressive functional behavior, their morphological fidelity is unclear. We believe our neurorobotic model is novel in that its behavioral transitions are due to a combination of descending commands and ascending sensory feedback, modeling particular pathways that support locomotion in the animal [68]. As such, the purpose of this work is not to replace reference [37], but to investigate certain insect neuromechanisms with a greater degree of detail than in reference [37].

In this manuscript, we present the development of our dynamic neuromechanical model of the femur-tibia (FTi) and coxa-trochanter (CTr) joints to explore the mechanisms used by the nervous system to control locomotion. We based our network on previous mappings of the NSI connections to the SETi in stick insects, then expanded it based on hypotheses grounded in experimental data. We validate the model's ability to replicate known motor responses to fCO stimulation, then selectively inhibit groups of position and velocity sensory neurons and observe changes to the joint's reflex action in mechanically decoupled and coupled cases. We combined this model of FTi reflex action with a previously developed stepping subnetwork [37] to produce 'sideways stepping' [30, 34]. Our findings suggest that input from the desDUM neurons to the motor control neurons and fCO afferents together sustain steady locomotion which can be initiated or halted by brief, transient descending signals from the head ganglia. Excitation of the CPGs and MNs by the desDUM enables stepping rhythm, while inhibition of parts of the fCO afferents permits movements in the joint that support walking. Feedback from the CS to the desDUM then works to autonomously sustain locomotion in the absence of descending signals. These effects combine to form a 'positive' reinforcement feedback loop that maintains locomotion by altering local sensory feedback and providing drive to the motorneurons. Using this feedback loop, the mechanical test limb produces and maintains stepping. Interrupting this feedback loop halts stepping. Finally, we discuss the implications of our findings on how the function of low level control networks may simplify the form of descending signals necessary to control behavior, as well as how these findings could be applied to robotic locomotion control.

2. Methods

2.1. Neuromechanical simulation development

We initially constructed our simulation in Animatlab 2 [25]. A simplification of our network structure is shown in figure 1, and all common abbreviations are listed in table 1. A brief overview of the network is as follows: the desDUM neuron (black) receives excitation from a higher level system, which initiates walking by exciting the pattern generating networks (dark blue) and motor-neurons (MN, orange) in each joint of the leg and inhibiting sensory afferents to create reflex reversal in the FTi joint (cyan and purple). A single neuron is used to represent the biological population of desDUM neurons to simplify our model. The time constant of the desDUM neuron is large enough that this relatively brief input will maintain walking for a longer period as the membrane voltage slowly leaks (e.g. figure 9(b)). As the leg walks, proprioceptive feedback from the fCO is encoded by a

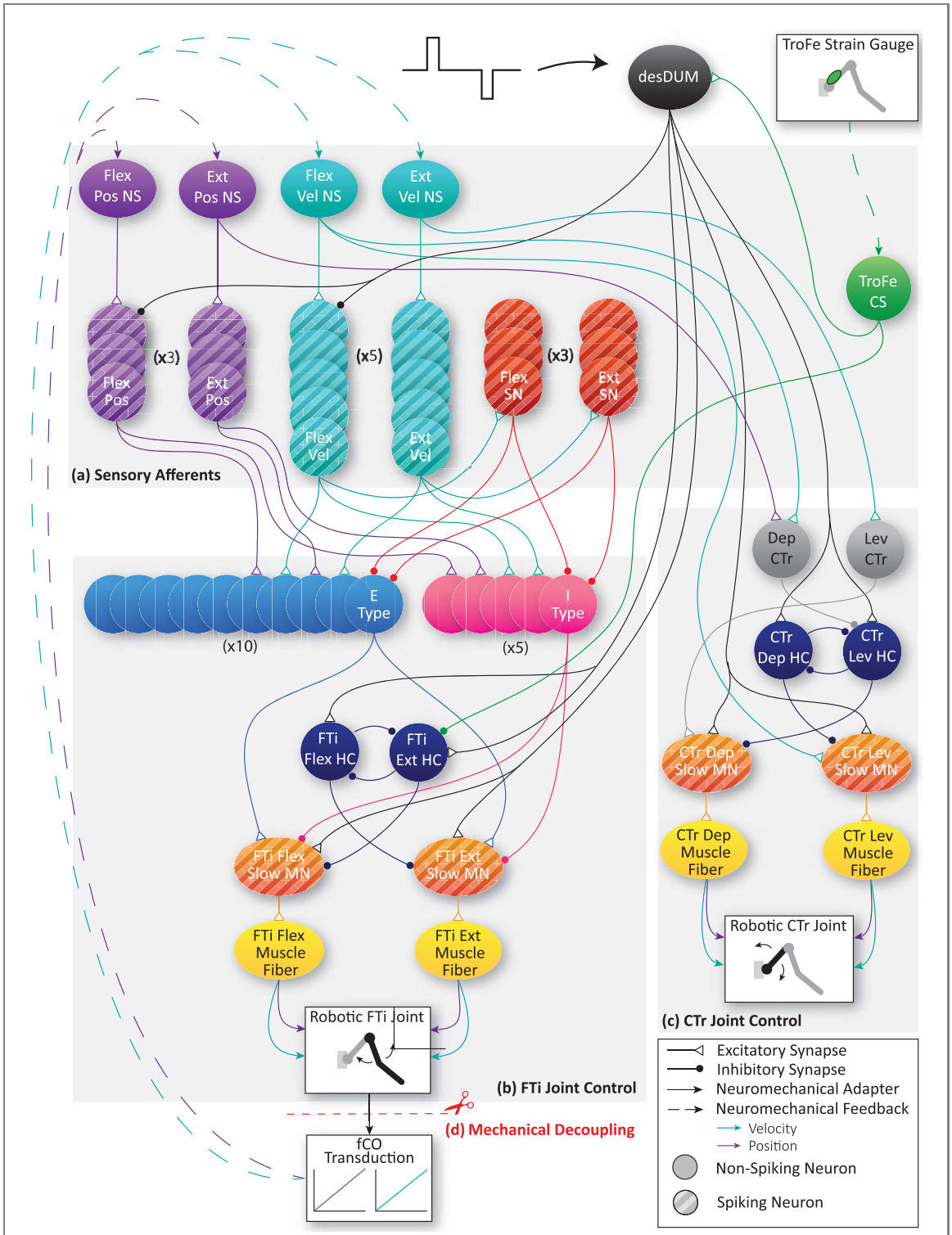

Figure 1. A simplified view of the simulation network. The desDUM neuron (black) initiates walking by exciting the pattern generating networks (dark blue) and motor-neurons (MN, orange) in each joint of the leg and inhibiting sensory afferents to create reflex reversal in the FTi joint. (a) The network receives position (purple) and velocity (cyan) proprioceptive feedback from the physical FTi joint or simulated counterpart, and strain feedback (green) from a strain gauge on the physical test leg positioned similar to the TroFe CS in the insect. To functionally replicate pre-synaptic inhibition, the proprioceptive feedback is initially received by a series of non-spiking sensory neurons which transmit the information to groupings of spiking sensory afferents. (b) E and I type NSI receive excitatory stimulus from the position and velocity sensory neurons, as well as a delayed inhibitory input from the velocity neurons transmitted through spiking interneurons (red). The outputs from these NSI synapse onto the slow MNs (orange) for the FTi joint, controlling the mechanical joint via non-spiking slow muscle fiber neurons (yellow). (c) The CTr joint functions similarly to the FTi joint control, with the sensory neurons modulating the pattern generators and MNs to coordinate with the FTi joint. (d) The connections between the joint output and the fCO were severed in some experiments, which we refer to as mechanical decoupling. More information regarding mechanical coupling and decoupling can be found in section 3.1.

Table 1. A list of the meanings for the commonly used abbreviations in the text.

Abbreviation	Meaning
VNC	Ventral nerve cord
fCO	Femoral chordotonal organ
RR	Resistance reflex
AR	Active reaction
NSI	Non-spiking interneuron(s)
NS	Non-spiking
SETi	Slow extensor tibiae motorneuron
MN	Motor neuron
desDUM	Descending dorsal unpaired median
FTi	Femur-tibia
CTr	Coxa-trochanter
CPG	Central pattern generator
CS	Campaniform sensilla
TroFe	Trochanterofemur
HC	Half-center

series of spiking sensory neurons. These sensory afferents affect the movement of the FTi joint via NSI, (blue and pink) synapsing onto the MNs. In the CTr joint, the proprioceptive neurons from the FTi joint directly stimulate the MNs and affect the pattern generating neurons through a CTr-specific pair of NSI (gray), which helps to ensure coordinated stepping in the leg. The system also encodes strain on the trochanterofemur (green), which contributes to stepping by resetting the FTi joint pattern generator, causing flexion inward during stance phase and providing continued excitation to the desDUM. This excitation sustains walking after the initial stimulus to the desDUM neuron abates. An inhibition of the desDUM from a higher level system is then sufficient to halt stepping.

The NSI and muscle fibers for each joint, as well as portions of the sensory neurons for the FTi joint, were modeled as non-spiking leaky integrators (solid in figure 1) [25]. As such, their membrane voltage, V, varies according to the differential equation:

$$C_{\mathrm{m}}\frac{\mathrm{d}V}{\mathrm{d}t} = I_{\mathrm{leak}} + I_{\mathrm{syn}} + I_{\mathrm{app}}, \tag{1}$$

where

$$I_{\mathrm{leak}} = G_{\mathrm{m}} \cdot (E_{\mathrm{r}} - V), \tag{2}$$

$$I_{\mathrm{syn}} = \sum_{i=1}^{n} G_{s,i} \cdot (E_{s,i} - V), \tag{3}$$

and I_{app} is an optional externally applied stimulus. Equations (2) and (3) define the leak and synaptic currents, respectively. In these equations, V is the current membrane voltage, G_{m} is the conductance of the cell membrane, C_{m} is the membrane capacitance, and E_{r} is the resting potential of the neuron. The instantaneous conductance of the ith synapse models the graded release of neurotransmitter in non-spiking synapses, and is a piecewise-linear function of the presynaptic neuron's instantaneous membrane voltage, V_{pre}:

$$G_{s,i} = G_{\mathrm{max},i} \cdot \begin{cases} 1, & \text{if } V_{\mathrm{pre}} > E_{\mathrm{hi}} \\ \dfrac{V_{\mathrm{pre}} - E_{\mathrm{lo}}}{E_{\mathrm{hi}} - E_{\mathrm{lo}}}, & \text{if } E_{\mathrm{lo}} \leqslant V_{\mathrm{pre}} \leqslant E_{\mathrm{hi}} \\ 0, & \text{if } V_{\mathrm{pre}} < E_{\mathrm{lo}}, \end{cases} \tag{4}$$

where $G_{\mathrm{max},i}$ is the maximum conductance of the synapse, E_{lo} is the synaptic threshold, and E_{hi} is the synaptic saturation. The synapse also has a reversal potential $E_{s,i}$, which varies depending on which neurotransmitter the synapse releases. For more details regarding the tuning of these parameter values, please see [73].

The motoroneurons and portions of the sensory neurons for both joints utilize the integrate-and-fire model for spiking neurons (striped in figure 1) [18]. These neurons exhibit leaky integrator behavior the same as the non-spiking neurons up until a threshold value, θ. Their membrane voltages evolve according to equation (1), with the added condition that:

$$\text{if } V = \theta, \quad \text{then } V(t) \to E_{\mathrm{r}}. \tag{5}$$

When a presynaptic neuron spikes, for each of its synapses, G_s is set to G_{max}, then decays according to the differential equation:

$$\tau_s \frac{\mathrm{dG}_s}{\mathrm{d}t} = -G_s, \tag{6}$$

where τ_s is the time constant of the synapse.

Our network controls the FTi and CTr joints of the leg, modeling the 'sideways stepping' preparation. This preparation is commonly used in both biological literature and modeling studies to explore NSI activity in stick insects [10, 30, 34]. Keeping our model within this scope allows for more direct comparison to these studies.

The following sections provide more detail on portions of the network.

2.1.1. Sensory afferents

The proprioceptive sensory afferents in the network are modeled after the layout for extension of the FTi joint presented in figure 1 of reference [57]. In this layout, the position and velocity of the joint are encoded by six position spiking sensory neurons (purple) and ten spiking velocity neurons (cyan). The velocity sensory neurons additionally synapse onto a set of six spiking interneurons (red), which provide delayed stimulus further downstream. Of the 16 position and velocity sensory neurons, half respond to fCO elongation (flexion) and half to fCO relaxation (extension). The firing rate of each sensory neuron is proportional to one of these four features: flexion position, flexion velocity, extension position, or extension velocity (figure 1(a)). To ensure that each sensory neuron's response is unique, each spiking

sensory neuron's membrane voltage includes a random fluctuation between −0.01 and 0.01 mV per simulation time step.

We also elected to include a non-spiking (NS) sensory neuron preceding the spiking neurons to model pre-synaptic inhibition. In the full figure diagram, these neurons are labeled 'Flex Pos NS', 'Ext Pos NS', 'Flex Vel NS', and 'Ext Vel NS' (figure 1). Please see table 1 for explanations of all abbreviations. These additional neurons allow us to produce multi-compartmental modeling of a neuron in Animatlab. Each group of spiking sensory neurons can be thought of as the synaptic terminals of the sensory afferent, whose dendrite and axon we model as the non-spiking sensory compartment. Distributing the feedback in this manner allows the spiking afferents to be inhibited during walking, preventing afferent communication with the NSIs. Meanwhile, other terminals of the same afferent retain the information they encoded for use in other portions of the network, e.g. influencing the timing of CTr rhythms [40]. This implementation functionally models pre-synaptic inhibition, which evidence suggests is commonly used by the nervous system to direct the flow of sensory information [80, 85].

In addition to proprioceptive feedback, the 'TroFe CS' neuron (green) encodes the strain of the trochanterofemur in the physical test limb. The inclusion of realistic simulated strain in our network had the potential to greatly complicate computation if confined to simulation. However, a much more straightforward approach is to collect real-time strain data from strain sensors on a physical limb. Combined with our desire to include mechanics to observe closed loop control, the inclusion of strain data to stimulate the desDUM neuron was best achieved through the inclusion of a mechatronic limb in our model. The network uses this stimulation to maintain walking by exciting the desDUM neuron, as well as entraining the FTi pattern generator. The onset of strain on the limb signifies the beginning of stance phase, so the strain neuron encourages the FTi joint to flex inward by inhibiting the extension half of the pattern generating neurons. In the insect, afferent responses to strain may reflect the amplitude of cuticle bending, the rate of bending, or both [86, 87]. To reflect this phenomenon, we implemented a filter that causes the sensor to adapt to bending measurements over long time periods and leads to a rate-based encoding of bending. A more in-depth description of this filter can be found in references [37, 75].

2.1.2. Non-spiking interneurons (NSI)

In the NSI portion of the network, the 10 E (excitatory; light blue) and 5 I (inhibitory; pink) type NSI receive excitatory stimulus from the position and velocity spiking sensory neurons, as well as delayed inhibitory input from the velocity neurons mediated by the spiking interneurons. We defined the layout and conductance strengths of the synapses between the sensory neurons and the NSI according to the relative values given in figure 11 of reference [57], as well as the recorded responses to similar stimuli presented in figure 2 of reference [57], figure 4 of reference [65], and figures 3.27–3.30 in reference [2]. Table 2 summarizes the reactivity of each NSI to sensory stimuli, as well as the corresponding literature reference. The exact response of each NSI to stimuli is presented in figure 2. Since the exact conversion between fCO stretch and neural activation has not been characterized, we arbitrarily chose a stimulus strength of 5 nA applied to the sensory neurons over 3.25 s. The stimulus ramps up to and down from the hold current over a period of 0.25 s. Because our physical limb is about 5 times larger than the stick insect, dynamic scaling suggests that the length of the stimulus should be about 5 times longer [43].

Table 2. A table summarizing the response of each NSI in our model to modulation by the different proprioceptive sensory neurons, along with the references to the corresponding biological data.

NSI	Responds to						Source
	Position		Velocity		SN		
	Flex	Ext	Flex	Ext	Flex	Ext	
E1	×		×		×	×	[57]
E2	×		×		×	×	
E3	×		×		×	×	
E4	×	×	×	×	×	×	
E5	×		×	×	×	×	
E6	×		×	×	×	×	
E7	×	×		×	×	×	
E8					×	×	[65]
E9	×		×		×	×	[2]
E10	×						
I1		×		×	×	×	[57]
I2	×		×	×	×	×	
I3	×	×			×		[2]
I4	×		×	×	×	×	[57]
I8					×	×	[2]

2.1.3. FTi joint control

The NSIs' outputs synapse onto the motorneurons (MN) (orange) via graded neurotransmitter release. To simplify network construction, we elected to only model the slow fibers of each muscle, and assumed each muscle would be activated by one slow motorneuron. The connection strengths of these synapses for extension were based on the relative values given in reference [57]. Connections to the flexor MN were also necessary to simulate full joint behavior and observe the effects of modulating the NSI; however, the network connections for the flexor slow MN have not been mapped in the insect. Functionally, Bässler *et al* recorded the forces of the extensor and flexor tibiae muscles in the stick insect for sinusoidal stimulus of the fCO and found that the forces varied in nearly equal and opposite ways (figure 3 in reference [8]). These results support the assumption that the flexor networks may resemble or mirror

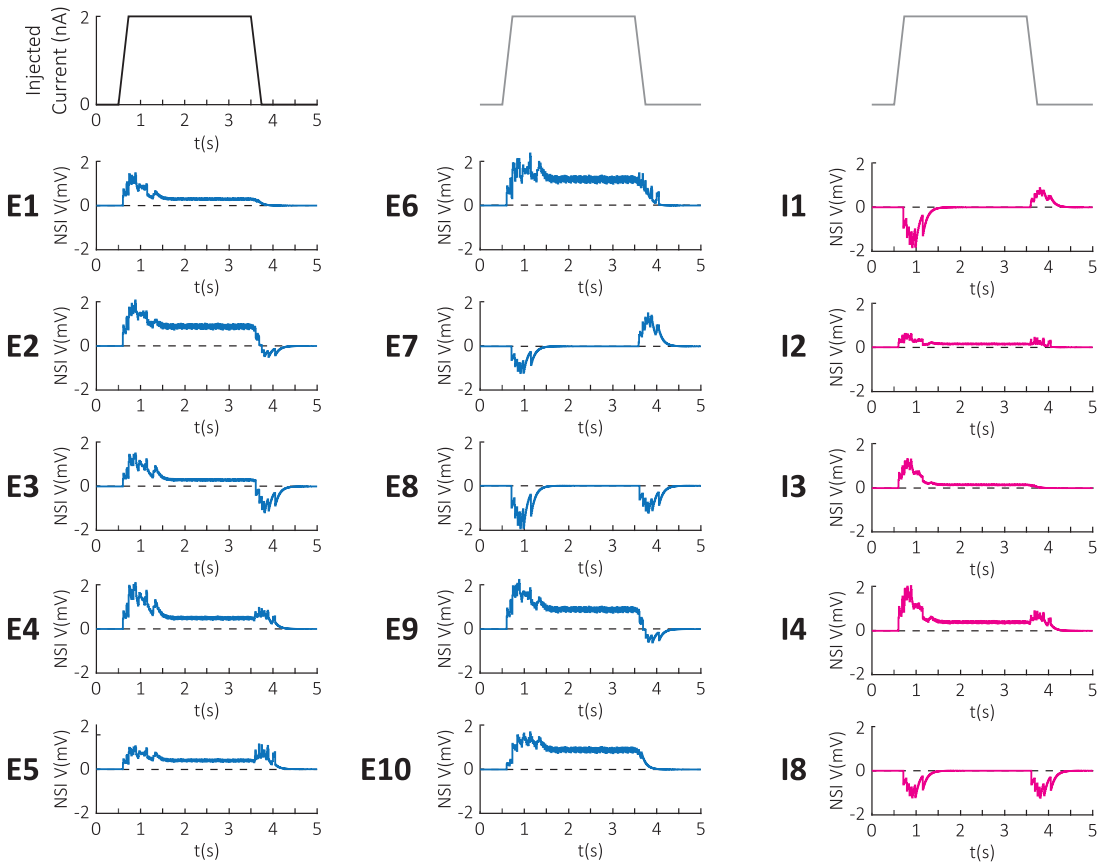

Figure 2. Each NSI's response to a ramp and hold stimulus in our simulation corresponding to fCO elongation (joint flexion). The interneurons are affected by a combination of active motion of the limb and sustained position. The exact nature and strength of the modulation (excitation, inhibition, or neither) varies depending on the category of interneuron. Table 2 summarizes the type of modulation for each NSI in our model, as well as the corresponding reference to the biological behavior. We took care to match the relative proportion of each to input to match responses from the literature. Our simulated NSI exhibit similar trends to the biological system with similar stimuli, showing that our model adequately simulates known biological behaviors.

those for extension. As such, we elected to include synapses between the NSI and the flexor MN that would produce a similar response to extension when given a mirrored stimulus, using similar strengths as in the extension synapses. Figure 3 shows that the responses of the extensor and flexor MNs in our network roughly mirror each other while the fCO is stretched and relaxed in a sinusoidal pattern.

To more directly interface with a simulated limb, we added a non-spiking neuron after the slow MNs as an analog for the insect's muscle fibers [25]. We set the time constant of these slow muscle fiber neurons to 2000 ms. The neuron then acts as a leaky integrator of synaptic inputs similar to a muscle [82]. The neuron's voltage is then used to command the position and velocity of a simulated limb through a pair of neuromechanical adapters. The limb's mechanics are governed by the equation of motion:

$$J \cdot \ddot{\theta} = \tau_{\text{ext}} + \tau_{\text{flex}} - k_{\text{spring}} \cdot \theta, \qquad (7)$$

where J is the moment of inertia of the limb, k_{spring} is the stiffness of the limb's parallel elastic elements and $\tau_{\text{ext,flex}}$ are the torques determined by the software to drive the joint at the speeds and to the positions indicated by the adapters. The precise tuning of these adapters can be found in reference [37].

To generate the cyclic rhythms for walking, each joint includes pattern generating neurons (dark blue) that synapse onto the MNs. These CPGs are modeled in the style of Daun-Gruhn [26] and Szczecinski *et al* [74], where each pair of non-spiking half-center (HC) neurons is coupled by mutually inhibitory connections. When each HC is given equal excitatory stimulus, this mutual inhibition creates repetitive bursting in the CPG, forming a HC oscillator. In our model, the neurons receive this excitatory input from the desDUM neuron to initiate or maintain walking [74]. The pattern generating neuron for flexion also receives excitatory stimulus from the strain sensory neuron, to ensure flexion of the FTi joint during stance phase. Since the pattern generating neurons create rhythmic motion in the MNs by inhibition [20], the desDUM neuron also excites the MNs. The synapses between the desDUM neuron and the MNs have a threshold potential equal to their saturation potential at 1.5 mV, such that they switch between maximum conductance and 0. This functionality ensures that the desDUM neuron will only activate the MNs when its membrane voltage is over a

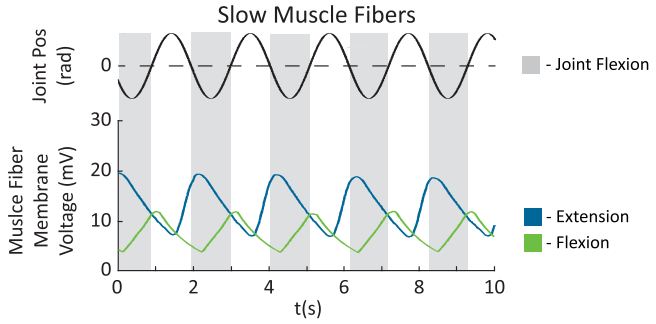

Figure 3. The response of the flexion and extension muscle fibers in our simulation to a sinusoidal stimulus of the fCO. In this preparation, the joint mechanics are unable to produce fCO stimuli (mechanical decoupling). The membrane voltages of each neuron exhibit similar excitation behaviors during the joint's corresponding motion (e.g. the extension fiber during extension). During the opposite motion, the voltages return to a similar rest value. This behavior aligns with the recorded behavior in reference [8].

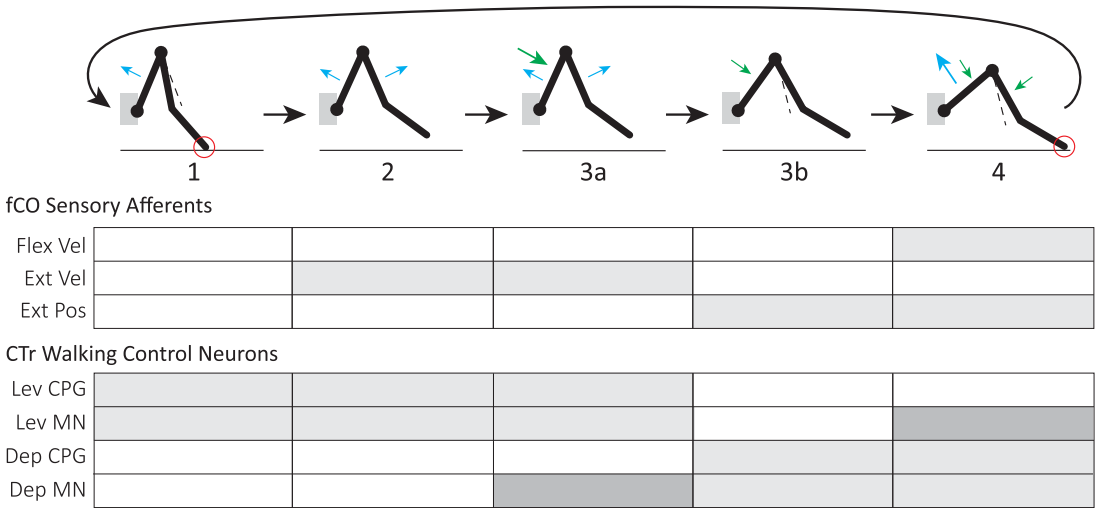

Figure 4. In our network, different motions for walking activate fCO afferents, which alter the response of the CTr joint's walking control neurons to ensure coordinated stepping in the leg. At each part, the sensory afferents and walking control neurons that are currently active are shaded in gray. If conflicting directions of neurons are active at the same time, the neurons that are dominant (i.e. correspond to current motion of the leg) are shaded darker. A more detailed description of each part depicted by these graphs can be found in the body text.

set point, and will do so regardless of the amount over that threshold. This activation helps to keep motion stable during walking by preventing over-saturation of the MNs. The synapses between the desDUM and the pattern generating neurons have a similar 1.5 mV threshold, but still allow for proportional stimulation up to 20 mV.

2.1.4. CTr joint control

Control of the CTr joint is similar to that of the FTi joint, with the proprioceptive feedback ensuring correct timing and correspondence between CTr joint motion and FTi joint motion for successful stepping. Such interjoint coordination mechanisms have been identified previously in the various insects [17, 39, 40]. We based a stepping cycle on the states outlined in figure 3(A) in Ekeberg *et al* (reference [30]), which we interpreted into four major parts (figure 4):

1. At the end of stance phase, with the FTi at the posterior extreme position (PEP), the CTr levates.
2. Once the foot is no longer loaded, the FTi extends as the CTr continues to levate.
3.
   a. After a slight delay, but while the FTi joint is still encoding a flexed position, the CTr depresses.
   b. Eventually, the FTi joint extends past the equilibrium position for the joint and enters the range encoded as an extended position, possibly reaching the anterior extreme position (AEP) and halting motion. The CTr continues depressing regardless.
4. Once the foot makes contact with the ground again, the FTi begins to flex while the CTr levates slightly in response to FTi flexion. The leg should stay depressed enough to maintain good contact

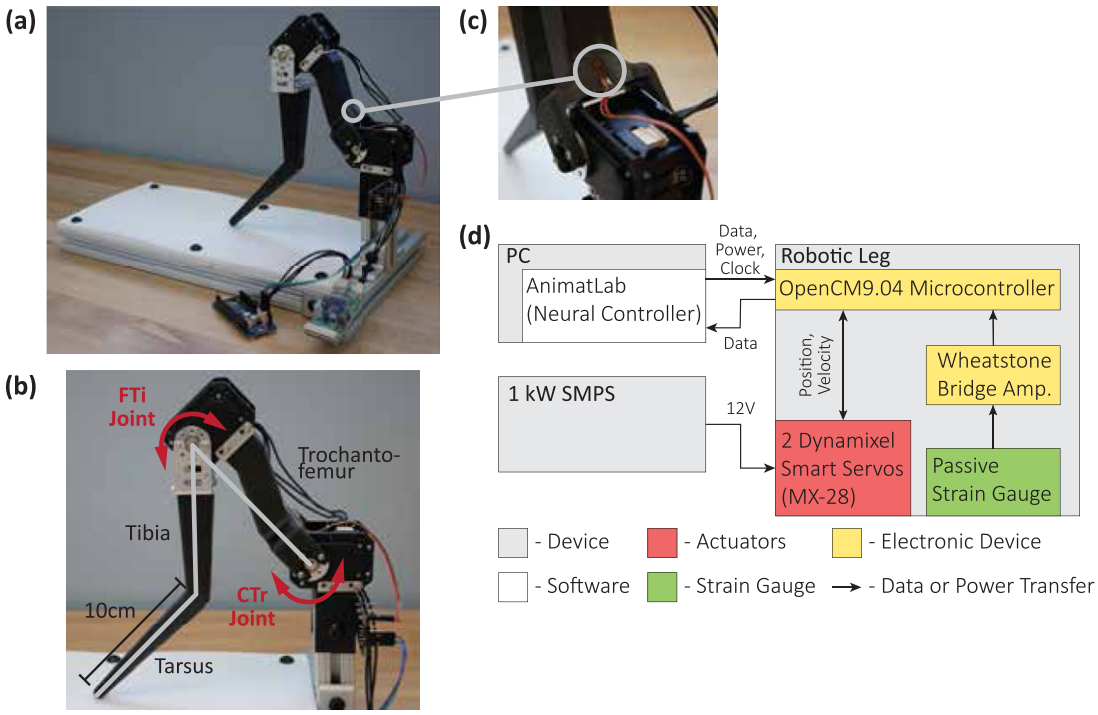

Figure 5. In order to include strain in our network in a straightforward way, we constructed a mechanical test limb which the network would direct. (a) A picture of the full test platform. (b) A magnified view of the leg, with anatomical components and directions of movement labeled. (c) Magnified view of the strain gauge, placed as an analog to the group 3 and 4 dorsal CS [88]. (d) Diagram illustrating the power and control systems of the test setup. A laptop computer runs the neural simulation, sending the appropriate data to the mechanical leg. The leg's micro-controller distributes actuator commands to the servomotors and collects sensory data from the servomotors and the strain gauge, which it then returns to the computer.

with the ground, until the FTi joint reaches its PEP.

Part 3 is split into 2 sub-parts to aid in categorizing the mechanisms behind the motion defined by the part. Previous investigations of the CTr joint in the insect found that fCO stretch (FTi joint flexion) caused CTr levation, and fCO relaxation (FTi joint extension) caused CTr depression in both resting and active animals [39, 40]. While the strength of this reflex in the active animal was increased over resting, the reflex seemed to only depend on the rate of fCO stretch (i.e. velocity signals) and were unaffected by changes in magnitude. This suggests that the fCO afferents, particularly those that encode velocity, impinge upon both the CTr joint MNs and the pattern generating neurons. To replicate this effect, we included two NSI, called 'Dep CTr' and 'Lev CTr', to receive stimulus from the non-spiking sensory neurons and impinge upon the MNs and pattern generating neurons. The interneuron that mediates CTr depression, 'Dep CTr', receives stimulus from the flexion velocity and extension position afferents, and inhibits the pattern generator half that promotes levation. The flexion velocity feedback ensures that the pattern generator will attempt to depress the leg when the FTi joint is flexing (e.g. during stance phase, part 4). The extension position will create the same response when the joint is in extension regardless of joint movement direction, ensuring that the CTr joint will continue to depress if the FTi joint reaches AEP (part 3(b)). To make the CTr levate slightly during stance phase (part 4), the flexion velocity afferent also excites the levator MN directly. The 'Lev CTr' interneuron is excited by extension velocity and in turn excites the depressor motorneuron, ensuring the joint depresses as the FTi joint extends (part 3). The inherent time delay introduced by the feedback encoding and distributing along the synapses ensures the CTr can levate off of the ground enough to step, as is necessary for part 3(a). Figure 4 summarizes the sensory feedback during each part of the stepping cycle, as well as the resulting effect on the pattern generating neurons and MNs.

2.2. Physical test platform development

In order to include strain into the network without complex simulation and computation, we constructed a mechatronic test platform for the network to interface with. Figure 5 includes several images of the finished setup. Each joint of the test leg is actuated by Dynamixel MX-28 smart servos (Robotis, Seoul, South Korea), with the leg segments constructed out of a combination of extruded nylon composite with continuous carbon fiber support and aluminum Dynamixel brackets. Each leg segment is approximately 10 cm long. Small animals' motions are dominated by elastic [1, 41, 58, 81] and viscous [36] forces rather than inertial and gravitational

forces. Such relationships can be quantified by applying length-based scaling laws of the mass, viscosity, and elasticity of the leg and its joints and designing the robot's stepping motion to have the same period relative to its dynamics' time constants as the animal has [37, 69]. While the precise mechanics of the stick insect were not considered here, the stiff servos and their high viscous forces (i.e. motion with no 'overshoot' or vibration) operate in the same dynamical regime. Thus, the leg likely converts neural states into motion in a way similar to the insect.

For simplicity, the leg only includes the CTr joint and the FTi joint. The tibia-tarsus joint (TiTar) is fused to create one large segment, while the thorax-coxa (ThC) joint is removed by securing the CTr actuator directly to the base of the test setup (figure 5(b)). In lieu of the motion provided by protraction or retraction of the ThC joint during walking, the base of the setup is comprised of Teflon sheeting, allowing the tip of the tarsus to slip across the surface.

The strain gauge is located at the proximal end of the trochanterofemur (figure 5(c)). This corresponds to the location of the dorsal trochanteral CS (groups 3, 4) in the insect [88]. The strain gauge has its own custom Wheatstone bridge to amplify the strain signal. The OpenCM then converts the analog voltage signals into 12 bit digital values, which are processed in the manner described in section 2.1.1 before being transmitted to AnimatLab. This filter mimics the discharge dynamics of CS, and in practice continuously cancels any constant offset voltages, either due to constant strain or the tuning of the Wheatstone bridge, allowing the model to accurately determine when the leg enters stance phase.

The electronic schematic for the system is shown in figure 5(d). An OpenCM 9.04 microcontroller (Robotis, Seoul, South Korea) manages data transfer between the test platform and the simulation computer, an offboard laptop that runs the neuromechanical model in AnimatLab [25]. Communication between the network and the test platform is managed in the same manner as presented in reference [37], where the neural system and the test limb run in a closed loop in real time. States (position, velocity, strain) from the limb are converted into currents by network adapters, then applied to the non-spiking sensory neurons. AnimatLab simulates neural states until the next test platform update (i.e. every 20 ms), then states from the neural system (membrane voltages of the muscle fibers) are mapped to servo commanded positions and velocities and sent to the microcontroller. An Arduino program on the microcontroller sends these commands to the appropriate actuators to control their next state. This functionality was first developed as part of the Animatlab Robotics Toolkit [25, 71].

3. Results

3.1. 'Normal' behaviors with mechanical decoupling and coupling

To validate the performance of our NSI sub-network after construction, we performed experiments in simulation to observe the behavior of the joint in response to a ramp-and-hold stimulus of the fCO. For each of these tests, the network was given fCO stimuli (i.e. stretch or relaxation) by an 'input joint' actually completing the desired flexion or extension and feeding into the 'fCO transduction' block (figure 1(d)). The position and velocity feedback of this motion was passed from the fCO block to the sensory afferents via neuromechanical adapters, then used by the network to generate joint movement on the 'output joint'. From there, the 'output joint' either connected to the fCO block to create further fCO stimuli (mechanically coupled case), or the connections were omitted (mechanically decoupled case). The mechanically decoupled case is our analog to the preparations used in biological experimentation, while the mechanically coupled case demonstrates the hypothetical behavior of an intact limb. The exact connections that are removed to switch between coupled and decoupled are called out in figure 1(d).

In addition, we considered ramp-and-hold stimuli corresponding to both FTi flexion and FTi extension. Biological literature defines the AR as the inhibition of the extensor muscle in response to FTi flexion [27, 38, 55, 57, 68]. As a result, the responses of these neurons to ramp-and-hold FTi *extension* have not been recorded. We choose to include the FTi extension case as hypothetical behavior of the limb in coupled and de-coupled cases. We will predominantly consider the behavior of the flexion case in the following sections.

Figure 6 shows the slow MN and muscle fiber activity along with joint motion at baseline synaptic and membrane conductances in mechanically decoupled and coupled configurations. In the mechanically decoupled case, the limb rapidly extends in response to stimulus corresponding to fCO elongation (flexion). Once this stimulus releases, the muscle fiber voltage slowly leaks and the limb returns to its equilibrium position. This MN firing trend resembles that of the SETi as observed in figure 8 of reference [57]. Additionally, the corresponding motion from this firing pattern makes logical sense as part of the biologically observed RR; the limb receives sensory feedback for undesired flexion and attempts to counteract the motion by extending. The data from the mechanically coupled case (b) further supports this observation. With joint motion creating fCO stimuli, the extension and flexion muscle fibers exhibit similar voltages throughout the applied stimulus, and so the limb oscillates between small angles of flexion and extension. Additionally, the MNs in the network fire at

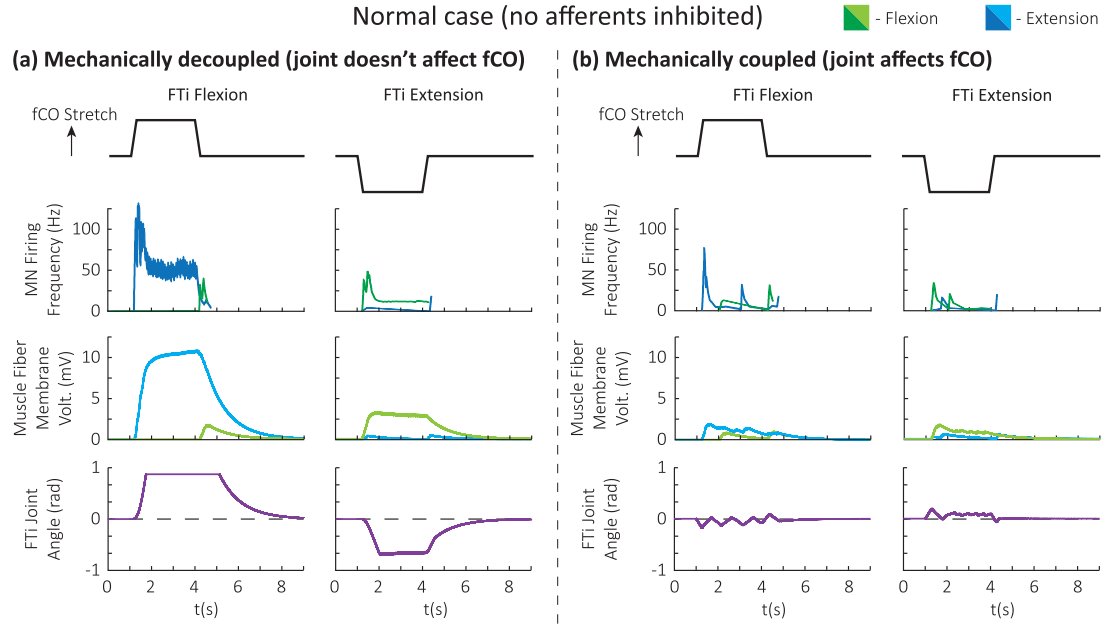

Figure 6. The response of the slow MNs, muscle fibers, and FTi joint in our simulation to a ramp stimulus corresponding to joint flexion (stretching of the fCO) and joint extension (relaxation of the fCO). (a) With joint movement unable to produce fCO stimuli (mechanically decoupled), the MN that opposes the motion encoded by the fCO predominantly excites and the joint extends to its limit in that opposing direction. (b) However, with the joint mechanically coupled to the fCO, the extension and flexion MNs fire at similar levels and the joint attempts to stay roughly at its neutral position. These results support the idea that the joint is attempting to resist movement in the baseline case, corresponding to the RR.

similar frequencies throughout their corresponding motion. Overall, the limb appears to exhibit behavior consistent with the RR in both the intact (mechanically coupled) and ablated (mechanically decoupled) cases.

3.2. Effect of sensory neurons on motion

Once the mechanically decoupled behavior of the joint was validated, we then tested the effects of inhibiting sensory afferents in response to joint flexion as described in Sauer *et al* in reference [55] on the decoupled model. To model such inhibition in our simulation without prematurely adding other neurons and synapses, we increased the time constants of each group of sensory neurons. This has the effect of decreasing the firing frequency in response to the same motion, which is functionally identical to changing the gain of the sensory neurons by altering their conductance [57]. We chose to test the system at time constants of 200 ms (normal value), 2000 ms, and 20 000 ms. A logarithmic range of inhibition produced the most distinctive changes between each case. Additionally, while inhibiting one 'polarity' of neurons (e.g. flexion), we kept the other polarity (e.g. extension) at their normal reactivity. Because the stimulus used for testing corresponds entirely to a flexed position, the extension position neurons are never stimulated. As such, we did not consider any combinations involving inhibition of the extension position neurons. We considered six types of test cases: one control case, three in which we inhibited a single polarity of either data type, and two in which we inhibited the flexion position group and one velocity group. This resulted in 15 total test cases. The input stimulus was the same ramp-and-hold corresponding to joint flexion used in section 3.1. A joint extension stimulus was not considered due to the lack of animal data for comparison.

Figure 7 shows the mechanically decoupled joint motion of the system in response to fCO stretching for various combinations of sensory neuron inhibition. The baseline case is outlines in red in the center of the figure axes for comparison. Beginning with the velocity axes of the graph (x-axis), inhibiting one of the velocity neuron groups on their own does not have a visible effect on the motion of the limb. However, combining this inhibition with that of the flexion position neurons produces a much more pronounced result. In all cases, the joint's resulting extension is less than half of that of the baseline. For the combination of flexion position and flexion velocity, the post-stimulus return to equilibrium is additionally more rapid, which results in a degree of overshoot into flexion. As the flexion position inhibition increases, the effect becomes more pronounced, with the cases involving high inhibition of flexion position and velocity resulting in little-to-no reaction to joint flexion.

This mechanically decoupled response resembles motion characterizing the AR; the joint is allowed to flex and even assisted in the motion. Figure 8(a) further explores the activity of the FTi neurons during these cases. In the mechanically coupled case, the activity of all of the MNs are diminished throughout

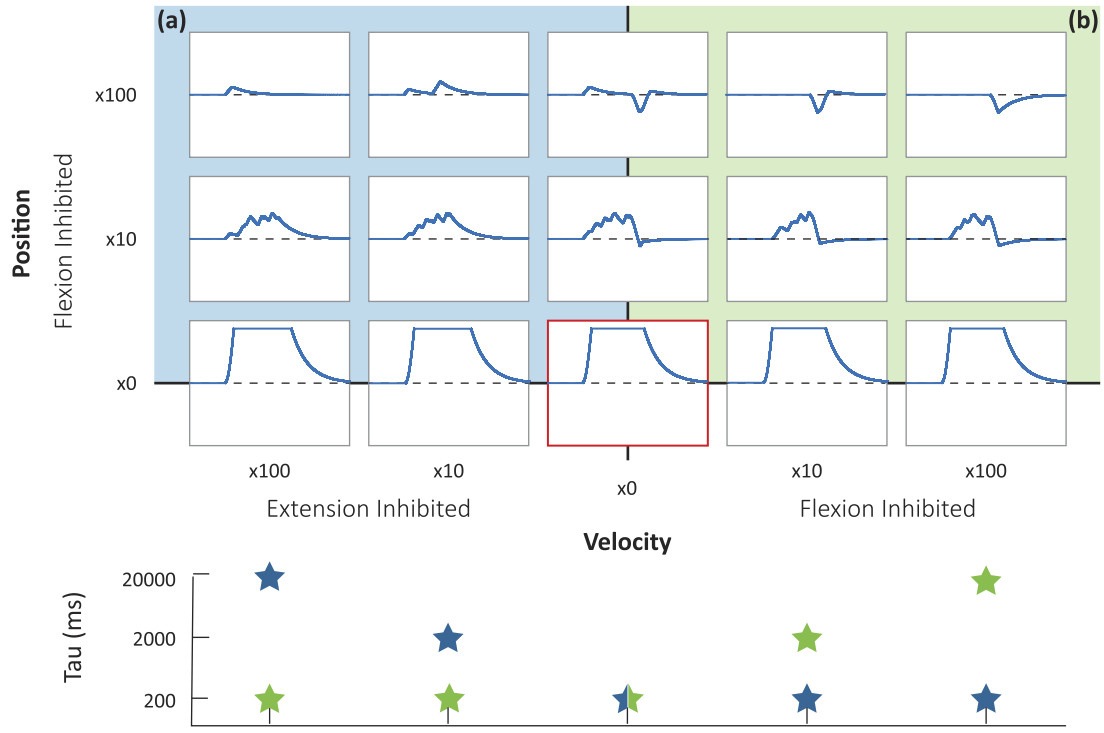

Figure 7. The joint response of the mechanically decoupled configuration of the simulation for increased time constants (corresponding to neuron inhibition) of various combinations of the sensory neurons. The stimulus used in these tests is the same as used in figure 6 corresponding to FTi flexion. The instance outlined in red corresponds to the baseline case explored in figure 6(a). In the left quadrant (blue), the flexion position and extension velocity groups are inhibited, and for the right quadrant (green), flexion position and flexion velocity are inhibited. While increasing the time constant of one velocity polarity (flexion, extension), the other was kept at baseline values. Because the stimulus corresponds entirely to flexion, the extension position neurons were omitted from testing. The bottom graph shows the specific time constants used for each level of inhibition of each polarity.

flexion. This result supports the idea that inhibiting a combination of flexion position and velocity sensory neurons could underlie the AR [27].

Because the extension sensory neurons are unaffected by this combination of inhibition, the system still produces a RR against unintended joint extension (figure 8(b)). The biological fidelity of this behavior is presently unknown, as the AR has been traditionally characterized only in terms of FTi flexion; the MN activity during fCO stimulation corresponding to an extended position has not been recorded. It is possible, then, that the nervous system could inhibit the extension sensory neurons similar to how we have modeled inhibition of flexion sensory neurons, symmetrically silencing all of the sensory feedback to the NSI. Previous experimental results have shown that the NSIs receive continuous sensory feedback during other active behaviors such as searching [10], so achieving the AR by inhibiting *all* fCO afferents seems unlikely. As such, we have elected to model the AR by asymmetrically inhibiting the flexion sensory neurons for our network.

3.3. Positive feedback in initiating, sustaining locomotion

Our preceding tests were conducted on the NSI and the FTi sensory and motorneurons isolated in simulation. Once our data verified these lower level portions of the network, we conducted tests with the full network interfacing with a physical limb, in order to observe the effects of the positive feedback loops on initiating and sustaining locomotion. In each test, the only stimulus entering the network was that to the desDUM neuron. This stimulus was either excitation at the beginning of the trial via 10 nA of injected current over two seconds, inhibition at the end of the trial via −5 nA of injected current over one second, both, or neither. The network received some combinations of FTi position, FTi velocity, and TroFe strain feedback throughout the trials. For all trials, reflex reversal was achieved through asymmetrical inhibition of the flexion sensory neurons, rather than symmetrical inhibition.

Figure 9 shows the resulting activity from the baseline case. The externally applied stimulus at two seconds excites the desDUM neuron, beginning stepping in the limb. Each time the tarsus impacts the ground, the resulting spike in strain (green) depolarizes the desDUM neuron, counteracting the leak of the neuron and keeping the membrane voltage within a similar range of excitation to continue stepping.

Figure 10 shows the effects of both joint strain and desDUM modulation on stepping. Without strain excitation of the desDUM neuron (figure 10(a)), the leg will only step until the desDUM neuron voltage decays past a certain threshold. In our model,

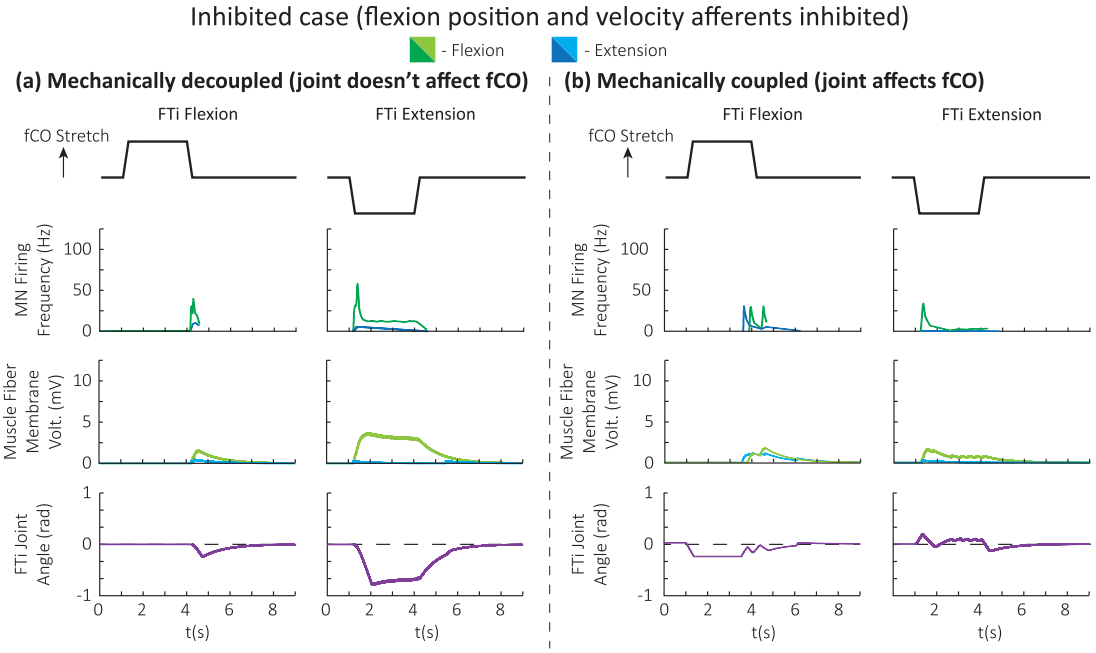

Figure 8. The response of the flexion and extension SETi and slow muscle fibers in our simulation to two different ramp stimulus while the flexion position and velocity neuron groups have been inhibited by increasing their time constants from 200 ms to 20 000 ms. (a) Response to stimulus without mechanical coupling. (b) Response to stimulus with mechanical coupling added back in.

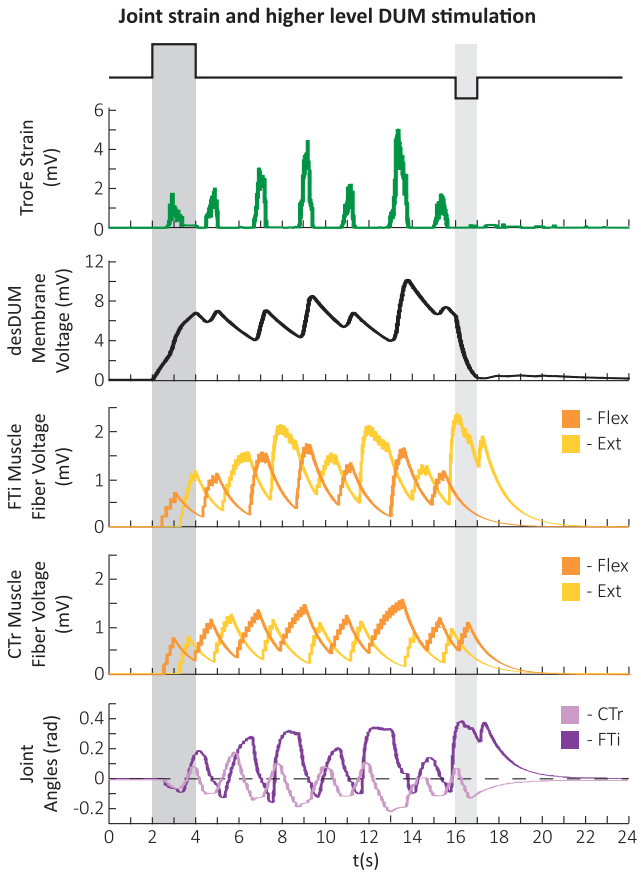

Figure 9. Through a combination of strain feedback and higher level desDUM neuron stimulation, our network can generate biologically plausible walking. In the 'baseline case', the desDUM excitation begins stepping, strain feedback maintains it, and desDUM inhibition ends it. See video S1 (https://stacks.iop.org/BB/16/065008/mmedia) for recorded results similar to this figure.

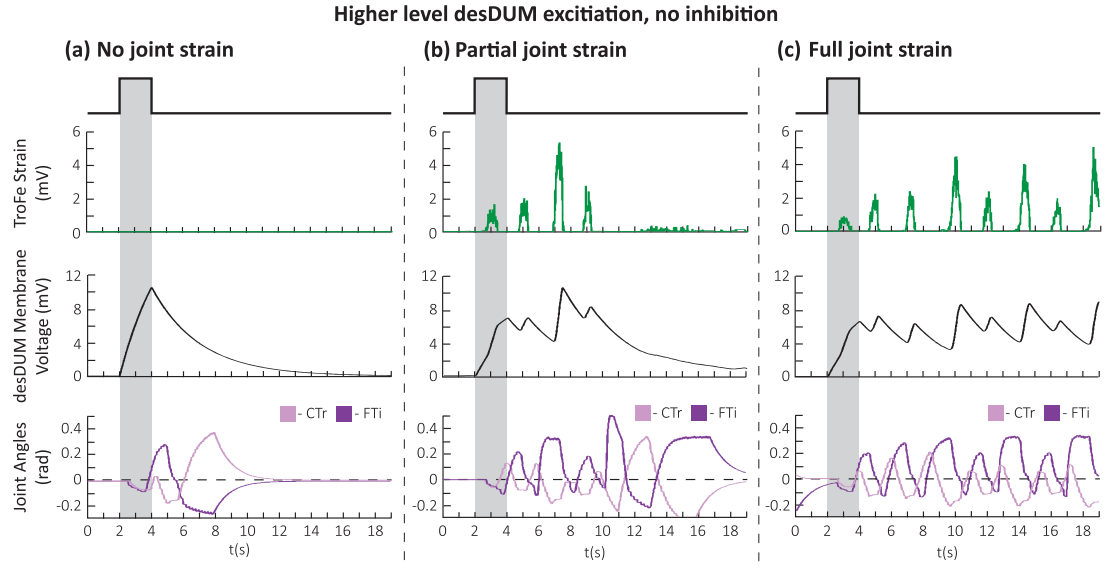

Figure 10. Strain feedback from the CS is integral to initiating and maintaining stepping. (a) If there is no strain feedback present, the limb will step until the desDUM neuron membrane voltage dips below a 1.5 mV threshold. (b) If the limb stops receiving strain feedback partway through stepping, the limb will move outside of normal parameters in an attempt to find the ground, then eventually cease stepping. (c) With strain working as intended and without a final inhibition of the desDUM neuron, the strain feedback will keep the limb stepping. In an ideal case, this could be sustained forever. See supplementary videos for recorded results similar to the no strain (S2) and partial strain (S3) cases.

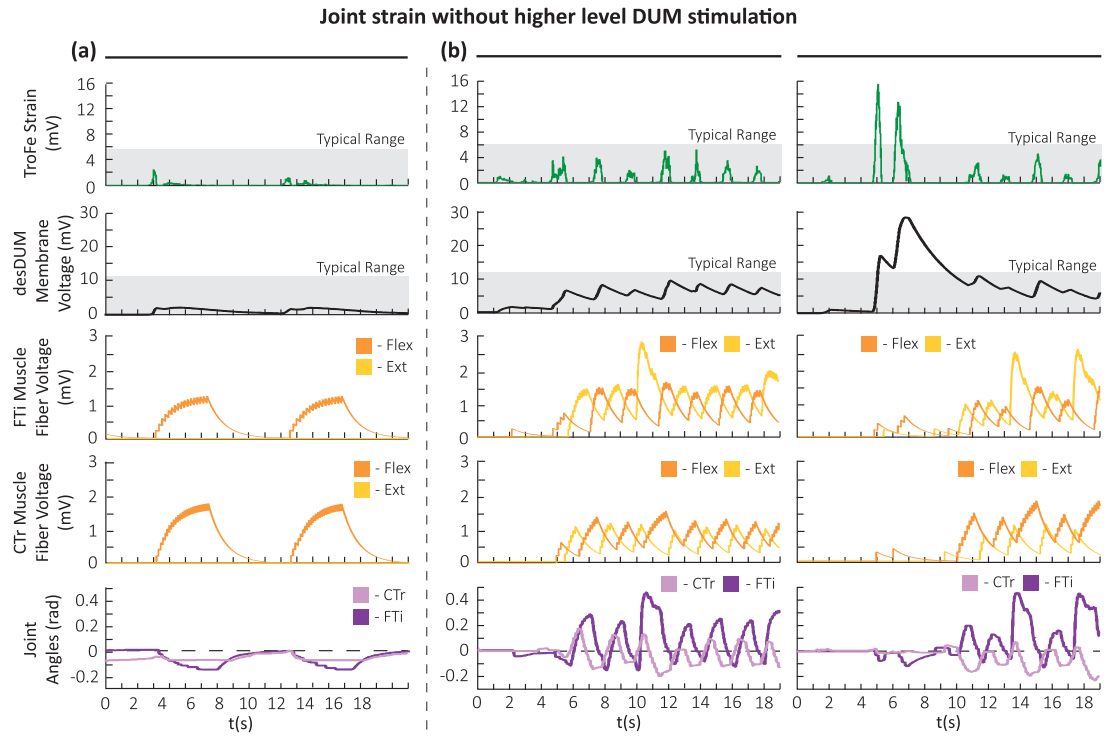

Figure 11. Depending on the magnitude, applied strain with no other stimulation of the desDUM neuron can produce varying joint motions. (a) For small strains, the MNs immediately saturating over the threshold will slightly move the limb. However, the pattern generators will not activate, so the limb will return to equilibrium rather than stepping. (b) For strains similar to or greater than those typical of walking, the desDUM neuron will excite the pattern generators, causing the limb to step long enough to generate the positive strain feedback to perpetuate motion. See supplementary video S4 for recorded results similar to (b).

this value was 1.5 mV, so this desDUM-only excitation resulted in two steps before the joints passively returned to equilibrium.

With strain providing positive feedback as intended, an inhibitory stimulus to the desDUM neuron is then necessary to hyperpolarize the membrane voltage enough to halt walking, which is applied at 16 s in our baseline case. Once applied, the joint passively returns to its equilibrium position over time. Without this inhibition, as in figure 10(c),

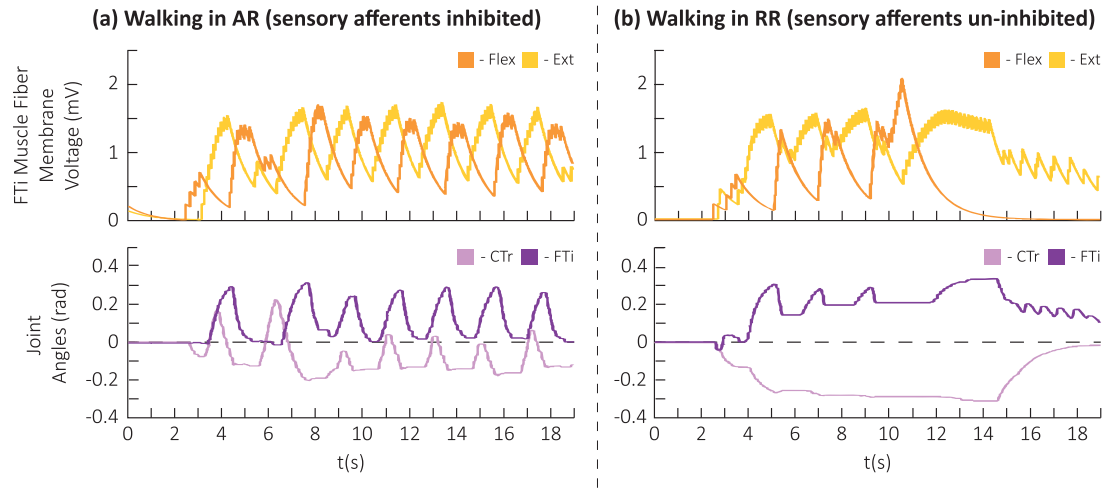

Figure 12. Inhibition of sensory afferents to initiate reflex reversal ensures proper stepping of the leg. (a) The AR enables rhythmic stepping by allowing motion in both directions. (b) If the network is kept in the RR during walking, the joint cannot move as intended due to the resistance generated by the NSIs. See supplementary video S5 for recorded results of walking in the RR.

the strain will continuously maintain the desDUM neuron voltage, allowing the leg to continue stepping. In our experimentation, we ran the system continuously for 50 steps. We observed that the stepping persisted, with a high degree of regularity between steps. Because the robot hardware intrinsically adds noise and feedback delays, the system's periodic motion is at least locally stable.

In cases where the network only receives strain feedback without higher level desDUM stimulation, the resulting limb motion can vary (figure 11). Small amounts of applied strain, as in figure 11(a), result in minimal MN activation and slight perturbation of the limb. This is because the activation of the desDUM neuron just barely passes over the threshold value for the synapses. The synapses for the MNs are set to saturate immediately at the threshold, so the corresponding MNs are fully activated by the strain stimulus. However, this voltage is not enough to begin rhythmic oscillation in the pattern generating neurons, so once the desDUM neuron voltage dips back below the threshold the MNs will decay back to equilibrium, halting motion.

Larger strains, meanwhile, can force stepping in the limb without higher level desDUM excitation (figure 11(b)). If the applied strain reaches levels similar to or larger than values characteristic of regular stepping, the excitation of the desDUM neuron will be large enough to excite the pattern generating neurons, kick-starting the positive feedback that will maintain excitation of the desDUM. Similar to the case in figure 9(c), this motion will likely continue until a large enough perturbation or inhibition disrupts the feedback cycle.

3.4. Reflex reversal effects during stepping

Finally, to observe the effects the reflex reversal could have on stepping, we conducted tests in which the limb stepped without the desDUM neuron inhibiting the sensory afferents identified in subsection 3.2. The results of these tests are presented in figure 12. When the sensory afferents are not inhibited, keeping the joint in the RR (figure 12(b)), the limb is unable to complete viable stepping. Instead, the limb drags itself along the walking surface in an oscillatory manner. Such behavior is likely due to the NSIs generating enough resistance to disrupt the desired range of motion of the joint. While the resulting motion is enough to temporarily sustain the positive feedback loop via limb strain, it is likely not viable for walking. This data supports our hypothesis that reflex reversal assists stepping by changing the allowable motions of the joint, allowing the pattern generators to dictate functional stepping.

4. Discussion

In this manuscript, we presented a neuromechanical model based on circuits that control insect FTi and CTr joints and including a physical test limb that is dynamically similar to the insect. The network is based on previously observed FTi extensor control networks in the animal, and was then expanded to include FTi flexor control and mechanisms to facilitate active walking in both leg joints. We performed experiments on the network in which we selectively inhibited groups of fCO sensory neurons and observed the FTi joint's response in both mechanically decoupled (as tested in animals) and mechanically coupled cases. Our findings suggest that inhibiting the flexion position and velocity sensory afferents can cause a transition from a RR to an AR in response to fCO elongation.

We also explored the higher level mechanisms the nervous system might use to transition into the AR

in the manner we describe, as well as initiate and sustain walking. We demonstrated that our network can initiate, maintain, and halt stepping in the physical limb with a combination of sparse descending commands mediated through a neuron representing populations of desDUM in the insect and biologically encoded strain feedback. More specifically, brief excitation of our desDUM neuron starts locomotion by exciting the MNs and pattern generators to prepare for stepping and inhibiting sensory neurons to reverse the FTi reflex. Strain feedback then reinforces motion by exciting the desDUM neuron with each step, maintaining its depolarization. If any of these components are absent, the leg cannot sustain viable stepping. If the system is intact, an additional descending command is necessary to halt stepping. These results support our hypothesis that two 'positive feedback' mechanisms, i.e. the AR and load feedback reinforcing stepping through desDUM excitation, are each necessary but insufficient to maintain locomotion.

4.1. Sensory afferent inhibition and reflex reversal

Our data concerning reflex reversal further supports the hypothesis of Sauer *et al* and Dreisang *et al* that descending commands may alter the control of motion by impinging upon the lowest level sensory afferents [27, 55]. In particular, the nervous system may alter the distribution of sensory information to portions of the network through pre-synaptic inhibition [80, 85]. Purposefully depriving portions of the control system of information to achieve a particular behavior seems counter intuitive from a robotics perspective. An engineer might attempt to implement this reflex reversal by collecting and distributing sensory information similarly no matter the context, then formulating context-dependent motor commands in response. This way, no sensory information is 'lost' to any part of the network at any given time. Why, then, might the animal nervous system utilize this strategy? It could be a matter of latency. Sending low level sensory information up to a central processor to interpret the data and send back context-dependent commands would create a time delay between the sensory feedback and the motor response. If the time delay is large enough, the system could become unstable, disrupting walking capability. Insects naturally have very short stepping periods, so the time needed to send information up to the cerebral ganglion and back down again may be inherently over the threshold for stability. Utilizing sparse descending commands to switch lower level systems into different states would reduce this latency, which could help ensure stable and effective walking.

Our findings also identified multiple possible combinations for sensory inhibition; the nervous system could asymmetrically inhibit only the flexion sensory neurons, or symmetrically inhibit all sensory neurons. As briefly discussed in section 3.2, the latter combination does not seem consistent with other active behaviors like searching [10]. Additionally, Hellekes *et al* found that MN responses consistent with the AR do not occur during backward walking (figure 5 of [38]). If sensory afferent inhibition is symmetrical and all sensory information is silenced, one would expect the extensor MN activity to decrease during stance phase whether the FTi joint flexes or extends during stance phase. However, when the FTi joint primarily extends (e.g. in the middle leg on the outside of a curved walking path, in the front leg during forward walking), extensor MN activity does not decrease, suggesting that sensory feedback signaling joint extension is present and sensory afferent inhibition may be asymmetrical. Thus, we hypothesize that the AR may represent an asymmetrical control mechanism in which motions in the intended direction (flexion) are permitted to occur, but motions in the unintended direction (extension) are resisted, as in the RR. If this is true in the animal, it suggests that the nervous system could define motor output in terms of constraining unwanted motions, rather than simply defining intended motion (e.g. joint angle or velocity) or active forces in the joint. These constraints would allow the joint to resist undesired movements from external forces while allowing assistive external forces to move the joint. We would then expect movement feedback to be asymmetrically inhibited throughout the leg to permit all leg joints to move as required for stance phase. In the case of our model, this could involve fCO feedback being applied to movement feedback for all joints of the leg, such as hair plate sensors at the ThC joint. Including these mechanisms in all leg joints might be one way to generalize our current model. However, additional biological experimentation is necessary to further explore this idea, in particular recordings of the behavior of the FTi MNs in response to joint extension during the AR.

4.2. Positive feedback versus reinforcement in the nervous system

We have emphasized the potential importance of positive feedback loops in managing walking throughout this manuscript. We use the term 'positive feedback' because it is often used in the literature [5, 61]. However, the control loops in our model (and possibly in the animal) starkly differ from the definition used in engineering, wherein the rate of change of a system's state is positively correlated with the value of the state. For example, while the AR is classically labeled as a positive feedback mechanism [5], it primarily reduces the resistance of the extensor to joint flexion. This behavior is certainly a reflex reversal from the case during the RR, in which flexion would activate the extensor. However, it is unlikely to lead to runaway exponential growth of flexion, and thus a more appropriate term may be warranted. The same could be said about the desDUM

neuron in our model, for which feedback from stepping contributes to further stepping. Instead, we prefer the term 'reinforcement' to describe such mechanisms. We believe that 'reinforcement' carries the same meaning as 'positive feedback', without the connotations it carries in engineering as being inherently unstable.

That said, reinforcement mechanisms appear to have functional benefits. As shown by our tests, reinforcement mechanisms enable sustained behavior given only transient inputs. Brief descending input signals can initiate a behavior (e.g. stepping), then the inputs added by the lower level feedback will attempt to maintain the behavior automatically. If the system seems to have 'failed' and the feedback is no longer present (e.g. no longer receiving load signals due to a limb missing the ground), the lack of further inputs will automatically halt the behavior. Similarly, strong enough feedback (e.g. a limb being strongly perturbed as a predator attempts to grab it) can rapidly initiate helpful behaviors (e.g. walking away from the threat) without any higher level inputs. A system based on contemporary engineering feedback may not perform as reliably, as feedback tied to the rate of change of the system state will naturally decay to zero as the system narrows in on the desired parameter. This settling will often occur quickly, ideally before the next time step. As such, a new input command would be necessary for each time step to maintain motion. The time step or the settling time could be increased to minimize the amount of high level commands necessary, but this would likely negatively effect the performance of the system. Regardless, having to frequently provide a higher level input signal greatly increases the computation required by the central processor, as well as increasing latency for the signal to travel. Therefore, sensory feedback driven reinforcement mechanisms may reduce control complexity by allowing for distributed, low level management of behaviors.

4.3. Broader conclusions and future work

In insects, the mechanisms of communication between the 'higher level command centers' (HLCC, e.g. the cerebral and gnathal ganglia) and the 'low level motor centers' (LLMC) in the VNC are largely unknown. Previous work has highlighted the distributed nature of neuronal control, as well as the role of the brain in producing adaptive locomotion [11, 51]. However, questions remain: what types of information are shared between the brain and VNC by descending neurons and ascending neurons? What do these pathways encode? What are their neuronal downstream targets? The present study begins to address these questions by modeling a specific system (i.e. the stick insect leg) while incorporating several decades of biological observations and data, including the higher-level modification of leg-local reflexes [27, 55], context-dependent activation of motor networks [44], and responses of desDUM neurons that may mediate such changes [68]. Our model may improve understanding the nervous system in general and lead to new robotic controllers. In particular, the fact that our largely low level network is capable of initiating and halting stepping without input from HLCCs suggests that the HLCC may simply define allowable or permitted movements, leaving the LLMC to formulate specific motor commands. This line of reasoning bears a similarity to the constraint-based joint control we hypothesized in subsection 4.1. Such a distributed control strategy could be a useful alternative for robotics applications in lieu of a complicated central processor directly commanding all motors. Specifically, descending signals could be provided by an operator or generated by a central processor, then the behaviors would be autonomously executed by the LLMC.

We have previously developed a six legged walking controller in reference [37], but this work explores portions of the control network with a greater degree of detail. As such, we will endeavor to apply our findings in this work to reference [37] to create a more in-depth network for six-legged stepping. Applying these mechanisms to the control of all six legs will require additional considerations, including a desDUM neuron that receives load input from all legs and subsequently excites all leg networks [68]. Embodying this network in a freely-walking robot will enable us to more closely examine how leg-local sensory information contributes to the maintenance of ongoing behaviors. For example, when an insect walks up to a gap in the substrate and fails to make ground contact with its front legs, it initiates a searching behavior [13, 78]. Part of this searching behavior is that the middle and hind legs slow their progress to allow the front legs time to find a foothold across the gap [13]. It is possible that such a change to forward progress is the result of decreasing reinforcement of desDUM activity when the front legs do not contact the substrate. Although the cerebral ganglion, particularly the central complex (CX), has been implicated in the control of the searching behavior, flies with missing CX substructures still halted upon reaching the gap [78], suggesting that while searching is directed by the cerebral ganglion, it may be initiated by local networks (e.g. desDUM neurons) or cerebral networks outside the CX. Using our robot, we will test the necessity and sufficiency of such networks in a level of detail not possible *in vivo*.

In addition, the role that reflex reversal may play in the movement of different pairs of legs is presently unclear. The present work models a middle leg, as biological preparations investigating the AR typically deal with the middle pair [10, 38, 68]. However, both biological experiments and modeling studies show that each set of legs plays a different role in locomotion [30, 35, 72, 76], meaning it will be important to consider reflex reversal in each of these roles when applying these mechanisms to a six-legged robot.

Experimental data from Hellekes *et al* show qualitatively similar AR behavior during middle and front leg stepping [38]. Additionally, Szczecinski *et al* hypothesized that each leg should undergo unique reflex reversals as the animal walks along paths of varying curvature [70, 72]. More data is necessary to determine the exact differences, if any, between the reflex reversals of each leg type.

Acknowledgments

This work was supported by the National Science Foundation (Grant 2015317 to NSS and RDQ and Grant 1704436 to RDQ).

Data availability statement

The data that support the findings of this study are available upon reasonable request from the authors.

ORCID iDs

C A Goldsmith https://orcid.org/0000-0002-3193-520X
N S Szczecinski https://orcid.org/0000-0002-6453-6475

References

[1] Ache J M and Matheson T 2013 Passive joint forces are tuned to limb use in insects and drive movements without motor activity *Curr. Biol.* **23** 1418–26
[2] Akay T 2002 The role of sensory signals for interjoint coordination in stick insect legs (Carausius morosus and Cuniculina impigra) *PhD Thesis* Universität zu Köln
[3] Akay T and Büschges A 2006 Load signals assist the generation of movement-dependent reflex reversal in the femur-tibia joint of stick insects *J. Neurophysiol.* **96** 3532–7
[4] Ayali A, Borgmann A, Büschges A, Couzin-Fuchs E, Daun-Gruhn S and Holmes P 2015 The comparative investigation of the stick insect and cockroach models in the study of insect locomotion *Curr. Opin. Insect Sci.* **12** 1–10
[5] Ulrich B 1988 Functional principles of pattern generation for walking movements of stick insect forelegs: the role of the femoral chordotonal organ afferences *J. Exp. Biol.* **136** 125–47
[6] Ulrich B and Büschges A 1998 Pattern generation for stick insect walking movements—multisensory control of a locomotor program *Brain Res. Rev.* **27** 65–88
[7] Ulrich B and Koch U T 1989 Modelling of the active reaction of stick insects by a network of neuromimes *Biol. Cybern.* **62** 141–50
[8] Ulrich B and Stein W 1996 Contributions of structure and innervation pattern of the stick insect extensor tibiae muscle to the filter characteristics of the muscle-joint system *J. Exp. Biol.* **199** 2185–98
[9] Berendes V, Zill S N, Büschges A and Bockemühl T 2016 Speed-dependent interplay between local pattern-generating activity and sensory signals during walking in Drosophila *J. Exp. Biol.* **219** 3781–93
[10] Berg E M, Hooper S L, Schmidt J and Bu A 2015 A leg-local neural mechanism mediates the decision to search in stick insects *Curr. Biol.* **25** 2012–7
[11] Bidaye S S, Bockemühl T and Büschges A 2018 Six-legged walking in insects: how CPGs, peripheral feedback, and descending signals generate coordinated and adaptive motor rhythms *J. Neurophysiol.* **119** 459–75
[12] Bidaye S S, Laturney M, Chang A K, Liu Y, Bockemühl T, Büschges A and Scott K 2020 Two brain pathways initiate distinct forward walking programs in Drosophila *Neuron* **108** 469–85
[13] Bläsing B and Cruse H 2004 Mechanisms of stick insect locomotion in a gap-crossing paradigm *J. Comp. Physiol.* A **190** 173–83
[14] Peter B and Burrows M 2004 Projection patterns of posterior dorsal unpaired median neurons of the locust subesophageal ganglion *J. Comp. Neurol.* **478** 164–75
[15] Peter B and Eder M 1998 Locust dorsal unpaired median (DUM) neurones directly innervate and modulate hindleg proprioceptors *J. Exp. Biol.* **201** 3333–8
[16] Ulrich B 1983 *Neural Basis of Elementary Behavior in Stick Insects* vol 10 (Berlin: Springer) p 169
[17] Bucher D, Akay T, DiCaprio R A and Büschges A 2003 Interjoint coordination in the stick insect leg-control system: the role of positional signaling *J. Neurophysiol.* **89** 1245–55
[18] Burkitt A N 2006 A review of the integrate-and-fire neuron model: I. Homogeneous synaptic input *Biol. Cybern.* **95** 1–19
[19] Busch S, Selcho M, Ito K and Tanimoto H 2009 A map of octopaminergic neurons in the Drosophila brain *J. Comp. Neurol.* **513** 643–67
[20] Büschges A 1998 Inhibitory synaptic drive patterns motoneuronal activity in rhythmic preparations of isolated thoracic ganglia in the stick insect *Brain Res.* **783** 262–71
[21] Büschges A and Gruhn M 2007 Mechanosensory feedback in walking: from joint control to locomotor patterns *Advances in Insect Physiology* **34** 193–230
[22] Büschges A, Rolf K and Ramirez J-M-M 1993 Octopamine effects mimick state-dependent changes in a proprioceptive feedback system *J. Neurobiol.* **24** 598–610
[23] Büschges A, Schmitz J and Bässler U 1995 Rhythmic patterns in the thoracic nerve cord of the stick insect induced by pilocarpine *J. Exp. Biol.* **198** 435–56
[24] Buschmann T, Alexander E, von Twickel A and Büschges A 2015 Controlling legs for locomotion—insights from robotics and neurobiology *Bioinspiration Biomimetics* **10** 041001
[25] Cofer D, Cymbalyuk G, Reid J, Zhu Y, Heitler W J and Edwards D H 2010 AnimatLab: a 3D graphics environment for neuromechanical simulations *J. Neurosci. Methods* **187** 280–8
[26] Daun-Gruhn S 2011 A mathematical modeling study of inter-segmental coordination during stick insect walking *J. Comput. Neurosci.* **30** 255–78
[27] Driesang R B and Büschges A 1996 Physiological changes in central neuronal pathways contributing to the generation of a reflex reversal *J. Comp. Physiol.* A **179** 45–57
[28] Dürr V 2005 Context-dependent changes in strength and efficacy of leg coordination mechanisms *J. Exp. Biol.* **208** 2253–67
[29] Dürr V *et al* 2019 Integrative biomimetics of autonomous hexapedal locomotion *Front. Neurorob.* **13** 1–32
[30] Ekeberg Ö, Blümel M and Büschges A 2004 Dynamic simulation of insect walking *Arthropod Struct. Dev.* **33** 287–300
[31] Emanuel S, Kaiser M, Pflueger H J and Libersat F 2020 On the role of the head ganglia in posture and walking in insects *Front. Physiol.* **11** 135
[32] Farooqui T 2007 Octopamine-mediated neuromodulation of insect senses *Neurochem. Res.* **32** 1511–29
[33] Feng K, Sen R, Minegishi R, Dübbert M, Bockemühl T, Büschges A and Dickson B J 2020 Distributed control of motor circuits for backward walking in Drosophila *Nat. Commun.* **11** 1–17

[34] Fischer H, Schmidt J, Haas R and Büschges A 2001 Pattern generation for walking and searching movements of a stick insect leg: I. Coordination of motor activity *J. Neurophysiol.* **85** 341–53
[35] Full R J, Blickhan R and Ting L H 1991 Leg design in hexapedal runners *J. Exp. Biol.* **158** 369–90
[36] Garcia M S, Kuo A D, Peattie A, Wang P and Full R J 2000 Damping and size: insights and biological inspiration *Int. Symp. Adaptive Motion of Animals and Machines* pp 1–7
[37] Goldsmith C A, Szczecinski N S and Quinn R D 2020 Neurodynamic modeling of the fruit fly Drosophila melanogaster *Bioinspiration Biomimetics* **15** 065003
[38] Hellekes K, Blincow E, Hoffmann J and Büschges A 2012 Control of reflex reversal in stick insect walking: effects of intersegmental signals, changes in direction, and optomotor-induced turning *J. Neurophysiol.* **107** 239–49
[39] Hess D and Büschges A 1997 Sensorimotor pathways involved in interjoint reflex action of an insect leg *J. Neurobiol.* **33** 891–913
[40] Hess D and Büschges A 1999 Role of proprioceptive signals from an insect femur-tibia joint in patterning motoneuronal activity of an adjacent leg joint *J. Neurophysiol.* **81** 1856–65
[41] Hooper S L, Guschlbauer C, Blümel M, Rosenbaum P, Gruhn M, Akay T and Büschges A 2009 Neural control of unloaded leg posture and of leg swing in stick insect, cockroach, and mouse differs from that in larger animals *J. Neurosci.* **29** 4109–19
[42] Ijspeert A J 2014 Biorobotics: using robots to emulate and investigate agile locomotion *Science* **346** 196–203
[43] Jayaram K, Mongeau J-M, Mohapatra A, Paul B, Fearing R S and Full R J 2018 Transition by head-on collision: mechanically mediated manoeuvres in cockroaches and small robots *J. R. Soc. Interface* **15** 20170664
[44] Ludwar B C, Westmark S, Büschges A and Schmidt J 2005 Modulation of membrane potential in mesothoracic moto- and interneurons during stick insect front-leg walking *J. Neurophysiol.* **94** 2772–84
[45] Marder E, Bucher D, Schulz D J and Taylor A L 2005 Invertebrate central pattern generation moves along *Curr. Biol.* **15** 685R–99
[46] Matheson T 1997 Octopamine modulates the responses and presynaptic inhibition of proprioceptive sensory neurones in the locust Schistocerca gregaria *J. Exp. Biol.* **200** 1317–25
[47] Mentel T, Weiler V, Büschges A and Pflüger H J 2008 Activity of neuromodulatory neurones during stepping of a single insect leg *J. Insect Physiol.* **54** 51–61
[48] Pflüger H J, Duch C and Heidel E 2004 Neuromodulatory octopaminergic neurons and their functions during insect motor behaviour *Acta Biol. Hung.* **55** 3–12
[49] Ramirez J-M, Büschges A and Rolf K 1993 Octopaminergic modulation of the femoral chordotonal organ in the stick insect *J. Comp. Physiol.* A **173** 209–19
[50] Ridgel A L and Ritzmann R E 2005 Effects of neck and circumoesophageal connective lesions on posture and locomotion in the cockroach *J. Comp. Physiol.* A **191** 559–73
[51] Ritzmann R E *et al* 2012 Deciding which way to go: how do insects alter movements to negotiate barriers? *Front. Neurosci.* **6** 97
[52] Roeder T 2005 Tyramine and octopamine: ruling behavior and metabolism *Annu. Rev. Entomol.* **50** 447–77
[53] Scott R, Szczecinski N and Quinn R 2018 A synthetic nervous system controls a simulated cockroach *Appl. Sci.* **8** 6
[54] Ryckebusch S and Laurent G 1993 Rhythmic patterns evoked in locust leg motor neurons by the muscarinic agonist pilocarpine *J. Neurophysiol.* **69** 1583–95
[55] Sauer A E, Büschges A and Stein W 1997 Role of presynaptic inputs to proprioceptive afferents in tuning sensorimotor pathways of an insect joint control network *J. Neurobiol.* **32** 359–76
[56] Sauer A E, Driesang R B, Büschges A and Ulrich B 1995 Information processing in the femur-tibia control loop of stick insects—I. The response characteristics of two nonspiking interneurons result from parallel excitatory and inhibitory inputs *J. Comp. Physiol.* A **177** 145–58
[57] Sauer A E, Driesang R B, Büschges A, Ulrich U and Borst A 1996 Distributed processing on the basis of parallel and antagonistic pathways simulation of the femur-tibia control system in the stick insect *J. Comput. Neurosci.* **3** 179–98
[58] Saunders F, Trimmer B A and Rife J 2010 Modeling locomotion of a soft-bodied arthropod using inverse dynamics *Bioinspiration Biomimetics* **6** 016001
[59] Scharzenberger C, Mendoza J and Hunt A 2019 Design of a canine inspired quadruped robot as a platform for synthetic neural network control *Biomimetic and Biohybrid Systems* **11556** 228–39
[60] Schilling M and Cruse H 2017 ReaCog, a minimal cognitive controller based on recruitment of reactive systems *Front. Neurorob.* **11** 3
[61] Schmitz J, Bartling C, Brunn D, Cruse H, Dean J, Kindermann T, Schumm M and Wagner H 1995 Adaptive properties of 'hard-wired' neuronal systems *Verhandlungen der Deutschen Zoologischen Gesellschaft* vol 88, pp 165–179
[62] Schmitz J, Schneider A, Schilling M and Cruse H 2008 No need for a body model: positive velocity feedback for the control of an 18-DOF robot walker *Appl. Bionics Biomech.* **5** 135–47
[63] Selcho M, Pauls D, el Jundi B, Stocker R F and Thum A S 2012 The role of octopamine and tyramine in Drosophila larval locomotion *J. Comp. Neurol.* **520** 3764–85
[64] Sinakevitch I, Niwa M and Strausfeld N J 2005 Octopamine-like immunoreactivity in the honey bee and cockroach: comparable organization in the brain and subesophageal ganglion *J. Comp. Neurol.* **488** 233–54
[65] Stein W and Sauer A E 1998 Modulation of sensorimotor pathways associated with gain changes in a posture-control network of an insect *J. Comp. Physiol.* A **183** 489–501
[66] Stein W, Straub O, Ausborn J, Mader W and Wolf H 2008 Motor pattern selection by combinatorial code of interneuronal pathways *J. Comput. Neurosci.* **25** 543–61
[67] Stevenson P A and Spörhase-Eichmann U 1995 Localization of octopaminergic neurones in insects **110** 203–15
[68] Stolz T, Diesner M, Neupert S, Hess M E, Delgado-Betancourt E, Pflüger H-J and Schmidt J 2019 Descending octopaminergic neurons modulate sensory-evoked activity of thoracic motor neurons in stick insects *J. Neurophysiol.* **122** 2388–413
[69] Sutton G, Szczecinski N, Quinn R and Chiel H 2021 Neural control of rhythmic limb motion is shaped by size and speed (accessed 6 June 2021)
[70] Szczecinski N S, Brown A E, Bender J A, Quinn R D and Ritzmann R E 2014 A neuromechanical simulation of insect walking and transition to turning of the cockroach Blaberus discoidalis *Biol. Cybern.* **108** 1–21
[71] Szczecinski N S, Chrzanowski D M, Cofer D W, Terrasi A S, Moore D R, Martin J P, Ritzmann R E and Quinn R D 2015 Introducing MantisBot: hexapod robot controlled by a high-fidelity, real-time neural simulation *IEEE Int. Conf. Intelligent Robots and Systems* pp 3875–81
[72] Szczecinski N S, Getsy A P, Martin J P, Ritzmann R E and Quinn R D 2017 Mantisbot is a robotic model of visually guided motion in the praying mantis *Arthropod Struct. Dev.* **46** 736–51
[73] Szczecinski N S, Hunt A J and Quinn R D 2017 A functional subnetwork approach to designing synthetic nervous systems that control legged robot locomotion *Front. Neurorobot.* **11** 37
[74] Szczecinski N S, Hunt A J and Quinn R D 2017 Design process and tools for dynamic neuromechanical models and robot controllers *Biol. Cybern.* **111** 105–27
[75] Szczecinski N S, Zill S N, Dallmann C J and Quinn R D 2020 Modeling the dynamic sensory discharges of insect campaniform sensilla *Conf. Biomimetic and Biohybrid Systems* pp 342–53

[76] Tóth T I and Daun-Gruhn S 2015 A three-leg model producing tetrapod and tripod coordination patterns of ipsilateral legs in the stick insect *J. Neurophysiol.* **115** 887–906
[77] Tóth T I and Daun S 2019 A kinematic model of stick-insect walking *Physiol. Rep.* **7** 1–26
[78] Triphan T, Poeck B, Neuser K and Strauss R 2010 Visual targeting of motor actions in climbing Drosophila *Curr. Biol.* **20** 663–8
[79] Tsubouchi A, Yano T, Yokoyama T K, Murtin C, Otsuna H and Ito K 2017 Topological and modality-specific representation of somatosensory information in the fly brain *Science* **358** 615–23
[80] Tuthill J C and Azim E 2018 Proprioception *Curr. Biol.* **28** R194–203
[81] von Twickel A, Guschlbauer C, Hooper S L and Büschges A 2019 Swing velocity profiles of small limbs can arise from transient passive torques of the antagonist muscle alone *Curr. Biol.* **29** 1–12
[82] Wolf H 2014 Inhibitory motoneurons in arthropod motor control: organisation, function, evolution *J. Comp. Physiol.* A **200** 693–710
[83] Wolpert D M and Ghahramani Z 2000 Computational principles of movement neuroscience *Nat. Neurosci.* **3** 1212–7
[84] Yellman C, Tao H, He B and Hirsh J 1997 Conserved and sexually dimorphic behavioral responses to biogenic amines in decapitated Drosophila *Proc. Natl Acad. Sci.* **94** 4131–6
[85] Zill S, Schmitz J and Büschges A 2004 Load sensing and control of posture and locomotion *Arthropod Struct. Dev.* **33** 273–86
[86] Zill S N, Büschges A and Schmitz J 2011 Encoding of force increases and decreases by tibial campaniform sensilla in the stick insect, Carausius morosus *J. Comp. Physiol.* A **197** 851–67
[87] Zill S N, Dallmann C J, Büschges A, Chaudhry S and Schmitz J 2018 Force dynamics and synergist muscle activation in stick insects: the effects of using joint torques as mechanical stimuli *J. Neurophysiol.* **120** 1807–23
[88] Zill S N, Schmitz J, Chaudhry S and Büschges A 2012 Force encoding in stick insect legs delineates a reference frame for motor control *J. Neurophysiol.* **108** 1453–72